Journal of Cardiovascular Magnetic Resonance (2005) **7**, 705–716

ISSN: 1097-6647 print / 1532-429X online
DOI: 10.1081/JCMR-200065639

Taylor & Francis
Taylor & Francis Group

HOW DO I

How we perform cardiovascular magnetic resonance flow assessment using phase-contrast velocity mapping

PING CHAI, M.R.C.P. and RAAD MOHIADDIN, F.R.C.R., F.R.C.P., F.E.S.C.*

Cardiovascular Magnetic Resonance Unit, Royal Brompton Hospital, London, UK

Flow assessment is an integral part of the comprehensive evaluation of the cardiovascular system. Cardiovascular magnetic resonance is well suited for flow assessment due to its non-invasive, multi-plane imaging capability unrestricted by windows of access and its ability to measure blood flow and velocity. Phase-contrast velocity mapping for flow assessment has been incorporated in all commercial scanners. It is versatile, and with appropriate hardware, software and expertise, it should be accurate and reproducible. In this article, we briefly describe the technique and indications for its use in current clinical practice. We suggest some practical tips in using the technique and describe some of the potential sources of errors and ways to overcome them. Finally, we provide several clinical examples demonstrating how to use phase-contrast velocity mapping in a number of acquired and congenital cardiovascular conditions.

Key Words: Cardiovascular magnetic resonance; Flow assessment; Phase-contrast velocity mapping

1. Introduction

The fundamental function of the heart is to ensure adequate perfusion of the body's organ systems. Assessment of blood flow is thus an integral part of the overall assessment of the cardiovascular function. Cardiovascular magnetic resonance (CMR) techniques offer several advantages, including wide fields of view, unlimited by windows of access, and the ability to measure velocities through as well as in a selected plane. It is non-invasive and is associated with minimal risks. Several CMR techniques have been developed for flow measurement, including time-of-flight methods and phase flow imaging methods (1). Most commercial scanners now offer flow assessment with phase-contrast velocity mapping, a method that has been validated (2–5) and found to be reproducible and versatile (6, 7). A major advantage of CMR is its ability to provide both anatomic and flow data in a single study. In this article, we shall briefly describe the basic concept of this technique, the indications for performing flow quantification, as well as potential limitations of phase-contrast velocity mapping technique, but the main focus shall be on how we perform flow and velocity quantification with this technique in routine clinical CMR studies.

Received 11 January 2005.
*Address correspondence to Dr. Raad Mohiaddin, F.R.C.R., F.R.C.P., F.E.S.C., Cardiovascular Magnetic Resonance Unit, Royal Brompton Hospital, Sydney St., London SW3 6NP, UK; Fax: +44-20-7351-8816; E-mail: r.mohiaddin@rbh.nthames.nhs.uk

2. Basic concept

The magnetic resonance (MR) signal has 3 components, namely, frequency, amplitude and phase, all of which are used for image reconstruction. Conventional MR images represent regional signal amplitude at each pixel in the displayed image. Phase shift or phase-contrast velocity mapping techniques use velocity-induced phase shifts to distinguish flowing blood from stationary tissue. Protons (or spins) moving in the direction of a magnetic field gradient acquire changes in phase or phase shifts (8). The phase shift experienced by a moving spin is proportional to its velocity, the strength of the applied gradient, and the period of time that it moves within that gradient. Using an additional bipolar velocity-encoding imaging gradient, a known linear relationship between the velocity of moving spins and the phase shifts is created while stationary spins acquire zero phase shift.

Phase-contrast velocity mapping techniques available on commercial scanners are usually gradient echo acquisitions (9), such as the FLASH (fast low-angle shot) sequence on most scanners. The technique can also be implemented using other rapid imaging methods such as echo planar imaging (10). Usually, two acquisitions, a velocity compensated and a velocity encoded acquisition, are performed with an additional bipolar gradient added for the second acquisition. Phase reconstructions are produced for each of the images, following which the 2 phase images are subtracted pixel by pixel to produce the final velocity map (Fig. 1). The process of subtraction aims to remove any phase variations that are unrelated to flow. To suppress background

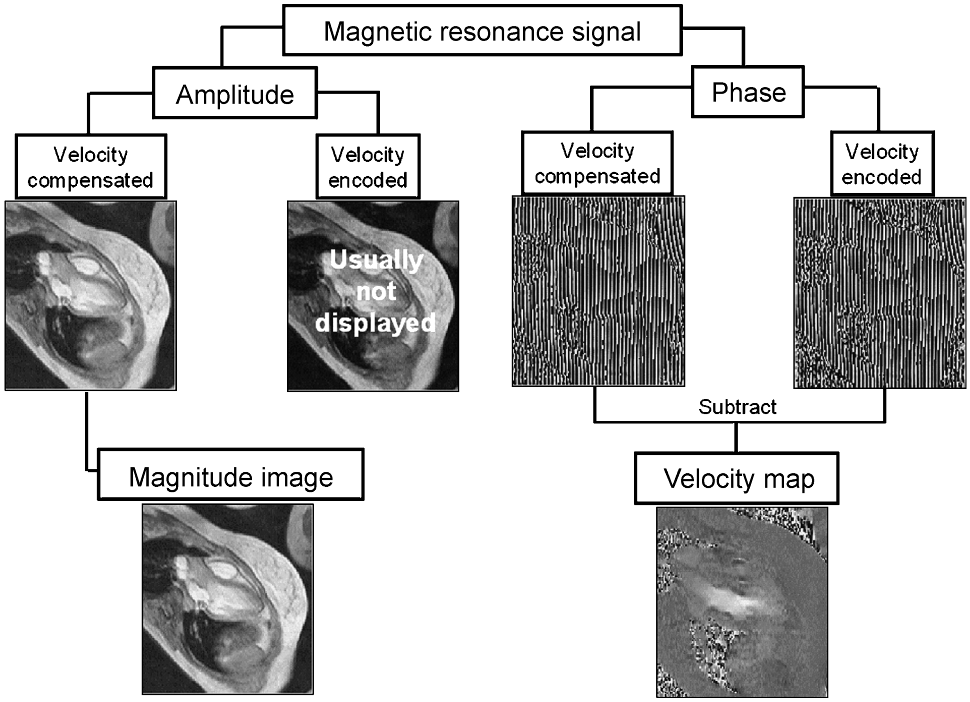

Figure 1. Schematic diagram showing phase-contrast velocity mapping. Pairs of velocity compensated (reference) and velocity encoded datasets are acquired. The latter datasets are subtracted to yield a velocity or phase map with pixel values linearly related to velocity.

pixels where the phase is random, such as air in the lungs, the phase subtraction image is multiplied with the conventional magnitude image. Phase shifts are measured as angles and their values are in the range of ± 180°. The constant that links velocity and phase angle is the velocity encoding or Venc, which specifies the maximum velocity that will be properly encoded by the sequence. The Venc adjusts the strength of the bipolar gradient so that the maximum velocity selected corresponds to an 180° phase shift in the data.

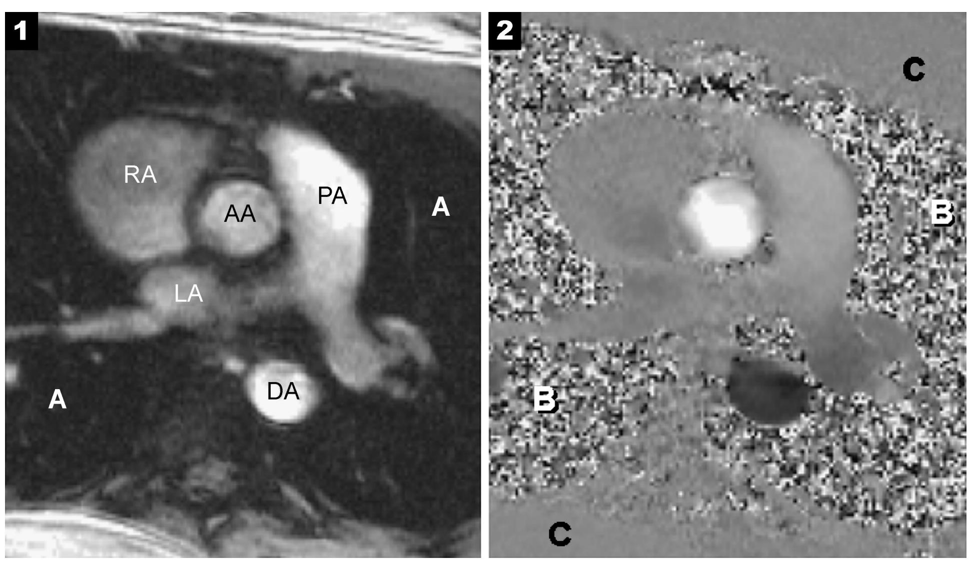

Figure 2. Typically, a phase-contrast velocity mapping acquisition produces 2 cine images, a magnitude (Panel 1) and a phase (Panel 2) cine. The magnitude image resembles a white blood gradient echo sequence. The phase image is presented as a gray-scale picture. In this through-plane acquisition perpendicular to the ascending aorta, cranial systolic forward flow in the ascending aorta (AA) is displayed as white, while caudally directed flow in the descending aorta (DA) is displayed as black. Ambiguous background noise from the lungs (A) appears as random black and white pixels (B) in the phase image. Stationary tissues from the chest wall (C) should appear as a uniform gray. PA indicates pulmonary artery; RA, right atrium; LA, left atrium.

Table 1. Indications for cardiovascular magnetic resonance flow measurement

- Valvular heart diseases
  - Valvular stenosis: determination of peak transvalvular velocity
  - Valve area planimetry
  - Valvular regurgitation: quantification of regurgitant volume and fraction
- Congenital heart diseases
  - Quantification of pulmonary to systemic flow ratio
  - Assessment of conduit stenosis
  - Assessment of severity of coarctation and collateral flow
  - Pulmonary arterial stenosis
  - Venous pathway stenosis
- Cardiac function
  - Left and right cardiac output determination
  - Mitral and tricuspid inflow patterns and volumes
- Vascular diseases
  - Identification of true and false lumens and points of entry in aortic dissection
  - Assessment of flow in arteriovenous fistulae
  - Severity of peripheral arterial stenosis
- Coronary flow
  - Coronary flow reserve measurement
  - Coronary bypass graft flow measurement

Adapted from Ref. (7).

Phase-contrast velocity acquisition usually generates 2 series of cine images: magnitude and phase images (Fig. 2). The magnitude images contain information about signal amplitude and resemble conventional white-blood gradient echo images. They are used for anatomic orientation. On the phase images, each pixel displays the mean velocity of the spins in that pixel. The phase images are therefore used for flow and velocity measurements (11). The encoded range of velocities is usually depicted as grayscale (or may be color-coded) and may be calibrated into velocity units by the display software. Tissues with stationary spins, such as the chest wall, are shown as a uniform gray. Pixels with spins moving in the velocity encoding direction are white, while those with spins in the opposite direction appear black. Pixels with arbitrary phase information (or noise pixels), such as those in the lung, appear as random white and black pixels.

2.1. *Indications*

We use phase-contrast velocity mapping in two ways, namely for flow quantification and peak velocity measurement. Table 1 list the major conditions in which this technique may be useful.

3. Using the technique in practice

Table 2 outlines the steps we usually employ for flow quantification with phase-contrast velocity mapping. Before commencing the CMR study, the patient should be positioned so that the region of interest is as close to the center of the magnet as possible to minimize the effects of Maxwell gradients on velocity acquisition. A good electrocardiographic tracing with prominent R wave spikes is a prerequisite. It is important to label velocity acquisitions with the intended slice location as this may be difficult to deduce subsequently.

We begin by defining the anatomy of the lesion using cine gradient echo imaging. This allows visualization of the vessel of interest and pathological flow, such as stenotic jets or turbulent flow, and the optimum imaging plane for velocity mapping can be defined. The various imaging parameters are then decided on before acquisition of the velocity images. Finally, the data is analyzed for peak velocity and/or volume flow, depending on the indication.

3.1. *In-plane versus through-plane velocity mapping*

On modern scanners, both in-plane and through-plane velocity mapping can be performed. In-plane velocity mapping is useful for visualizing the flow jet and estimation of peak velocities. With in-plane acquisitions, velocity encoding can be in one of two directions, represented vertically or horizontally in the acquired image. If one of these is encoded, it should be parallel to the direction of the flow in the vessel of interest, which can be achieved by in-plane rotation of the field of view.

Through-plane acquisitions are used for both velocity measurement and flow quantification. For accurate assessment, the imaging plane should be perpendicular to the jet or the vessel

Table 2. Proposed steps in performing magnetic resonance phase-contrast velocity mapping

1. Define anatomy and pathological flow with cine gradient echo imaging.
2. Decide imaging plane: through-plane for volume quantification, through-plane and/or in-plane for velocity measurement.
3. Decide on breath-hold or non-breath-hold acquisition.
4. Optimize field of view: alignment with flow or vessel of interest, minimize phase wrap artefacts.
5. Decide on electrocardiographic gating: retrospective or prospective.
6. Adjust parameters: number of frames/phases per cardiac cycle, repetition time, number of segments.
7. Set velocity envelope (Venc), and for in-plane acquisition, velocity encoding direction.
8. Acquire images.
9. Repeat above steps, adjusting imaging planes, Venc, and other parameters as necessary to achieve optimal image quality and flow data.
10. Data post-processing and analysis.

of interest. A high-velocity jet visualized by in-plane velocity mapping can be useful for locating a subsequent through-plane acquisition. However, in-plane acquisitions tend to underestimate the velocity of a narrow jet because of partial volume averaging or misalignment with the jet. Correctly located through-plane velocity maps are more reliable as long as the imaging plane transects the core of the jet just downstream of the orifice, at its point of maximum velocity. The jet core has coherent laminar flow and can be recognized as a central region of high signal surrounded by darker regions of turbulent flow on conventional gradient echo images (see Example 1), and it corresponds to the region of highest velocity on phase-contrast images. A series of cine and velocity acquisitions may be needed to locate the jet core. Some narrow jets, for example those of mitral, aortic and mild tricuspid valve regurgitation, lack a sufficiently coherent jet core for accurate phase-contrast velocity mapping.

3.2. *Electrocardiographic gating*

Retrospective gating is recommended for flow measurement. It gives coverage of the whole cardiac cycle and reduces artifacts due to eddy currents that may result from interruption of regular gradient application as in prospective gating. Arrhythmias such as atrial fibrillation can cause significant variation of cardiac cycle length, in which case prospective gating may have to be used.

3.3. *Breath-hold versus non-breath-hold acquisitions*

Phase-contrast velocity mapping can be performed with both breath-hold and normal respiration. Breath-hold acquisitions have the advantage of more precise location of scout images, as well as being much quicker. Using segmented FLASH sequences, parameters such as temporal resolution and number of views per segment can be adjusted to achieve a sufficiently short acquisition time. Scan time may also be reduced by decreasing the number of phase encoding steps (reduce the phase field of view) at the expense of introducing phase wrap artifacts but these are acceptable so long as they do not encroach into the region of interest. We usually perform breath-hold acquisitions for peak velocity measurements with breathing arrested at end-expiration. Breath-holding may, however, have physiological effects on blood flow (12).

With non-breath-hold techniques, usually sequential FLASH acquisitions, scan time is less of a consideration although it should still be taken into account for patient comfort. Higher temporal resolution can be achieved. We usually employ non-breath-hold acquisitions for volume flow measurement. However, irregular breathing patterns may result in excessive respiratory motion artifacts in some cases.

3.4. *Data analysis*

For peak velocity estimation, the images in the relevant phase of the cardiac cycle are used. For instance, in the case of aortic valve stenosis, the systolic images are analyzed. The phase images are examined for pixels with the highest encoded velocity in the central jet region. Most software packages provide this data automatically for a small region of interest (ROI) drawn on the phase images. Care should be taken not to include extreme pixels near the edge of a jet where artifacts can occur. For consideration in relation to traditional catheter investigation, pressure difference (ΔP) across a stenosis can be estimated by the modified Bernoulli equation:

$$\Delta P = 4 \cdot (\mathrm{V}_{\max})^2 \tag{1}$$

where $\mathrm{V}_{\max}$ is the peak velocity in meters per second.

For flow quantification, contours must be delineated around the internal border of the vessel of interest on all phase images throughout the cardiac cycle. This should preferably be done directly on the phase images. If edge definition of the vessel is poor on the phase image (usually because of low velocities), the ROI may be contoured on the magnitude images and subsequently transferred to the corresponding phase images. The ROI must be cross-checked on the phase images to ensure that they do not include noise or edge pixels. Some software packages incorporate automated contour detection, but the generated contours must always be checked thoroughly for accuracy. Mean flow is calculated as the area of the ROI multiplied by the mean velocity (13). The flow data for all the phases in a cardiac cycle are then integrated to give total flow per heart beat. A flow versus time curve can be plotted. Most software packages automatically compute data for stroke volume, cardiac output, and cardiac index.

4. Pitfalls and limitations

There are several potential sources of error that may compromise the accuracy of flow measurement with this technique. These sources of error may be inherent in hardware design, or may arise during image acquisition and/or data analysis. With improvements in modern scanner hardware designs, the largely vendor-specific hardware problems have been ameliorated. In the following paragraphs, we describe some of these sources of error and suggest ways of minimizing them.

4.1. *Mismatch of encoding velocity*

Precision of flow measurement depends, among other things, on how closely the specified Venc matches the true velocity in the region of interest. This is because quantification of flow and velocity are affected by noise. Noise is caused by random error of phases and becomes more pronounced with larger encoding velocities (14). If Venc is set too high, the range of flows imaged will encompass a limited number of degrees of phase shift, and the signal-to-noise ratio of the image will suffer. Noise affects peak velocity estimation more than flow

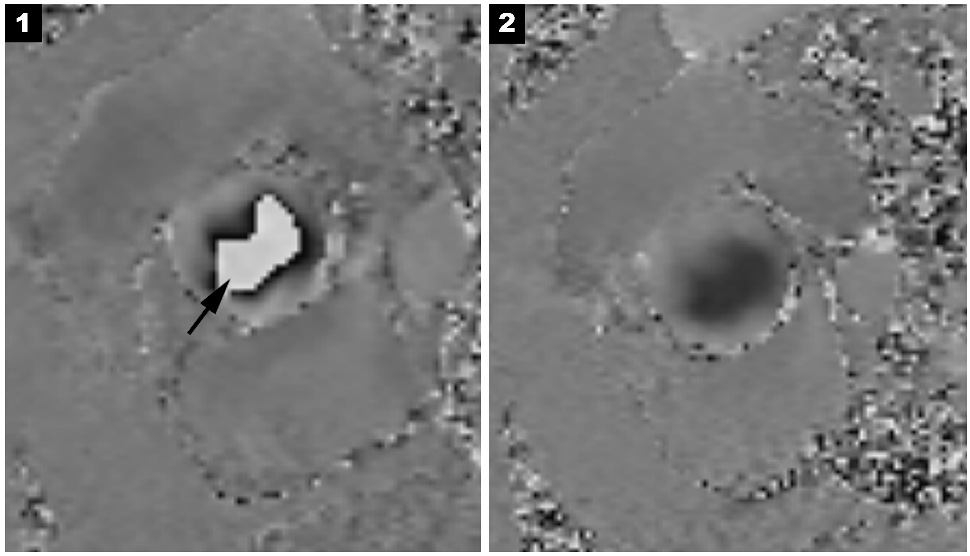

Figure 3. Phenomenon of aliasing. Through-plane velocity mapping of the aortic root in a patient with bicuspid aortic valve. Panel 1 shows the phase image at mid-systole with Venc set at 200 cm/s. Systolic forward is displayed as black, but in this image, white pixels (arrowed) appear where the peak velocities have exceeded the Venc and undergone more than 360° phase wrap. Panel 2 shows a second acquisition with Venc set at 300 cm/s, eliminating the aliasing effect. The actual peak velocity is 2.4 m/s.

quantification due to masking of the peak velocity by noise peaks. Ideally, the Venc should be set within 25% of the true maximal velocity in the region of interest.

If the encoding velocity is set lower than the true peak velocity, aliasing results (Fig. 3). This is due to a 360° wrap around of velocity information within a voxel. It can be detected in the phase images as voxels with signal intensities which are opposite to that of surrounding voxels in the same flow direction. Aliasing can be minimized simply by increasing the Venc during data acquisition. It can also be corrected manually during data analysis or using some software packages, but there is a limit to the velocity correction range that can be applied (15). We usually start out with breath-hold velocity map acquisition using a Venc setting which is an estimation of the true velocity based on clinical data and the findings on gradient echo imaging, such as orifice size and jet width. If aliasing occurs, we repeat the acquisition with a higher Venc setting until aliasing disappears.

In some patients with mixed valvular heart disease such as concomitant aortic valve stenosis and regurgitation, it may not be possible to obtain accurate estimations of peak velocity through the stenotic valve as well as regurgitant fraction in the same acquisition with one Venc setting. This is because the stenotic jet is of high velocity and requires a high Venc, which may underestimate the regurgitant flow. Conversely, regurgitant flow is of low velocity requiring a lower Venc setting, which will produce aliasing in the stenotic jet. In this situation, separate acquisitions with different Venc settings may have to be performed, and the data from the relevant parts of the cardiac cycle can then be integrated to give regurgitant volume and fraction. However, this method requires validation.

4.2. *Misalignment of imaging plane*

Measurements of flow and velocity are most precise when the imaging plane is orthogonal to the direction of flow. For through-plane acquisitions, every attempt should be made to align the image plane perpendicular to the vessel of interest for flow quantification or perpendicular to the direction of the jet for peak velocity estimation. Deviation of up to 20° is acceptable for flow measurement. An ovoid shape of an artery on the magnitude image usually indicates a gross misalignment of the imaging plane in through-plane acquisition. Peak velocity measurement may also be inaccurate with through-plane acquisitions if the imaging plane misses the region of the jet with the highest velocity. Several acquisitions at contiguous levels downstream along the jet may be required.

For in-plane acquisition, the direction of velocity encoding should be parallel to the direction of flow, which can be derived from the flow characteristics and vessel alignment on gradient echo imaging. This can be achieved by in-plane rotation of the field of view, or changing velocity-encoding direction. It is important to ensure that the imaging plane transects the plane of the jet and several acquisitions in different orientations may be necessary to achieve this. Velocity estimation of a narrow, mobile jet may be inaccurate due to movement of the jet in and out of the imaging plane.

4.3. *Inadequate temporal resolution*

Phase-contrast velocity mapping yields a series of images or frames containing anatomic and velocity information at different time points throughout the cardiac cycle. If the

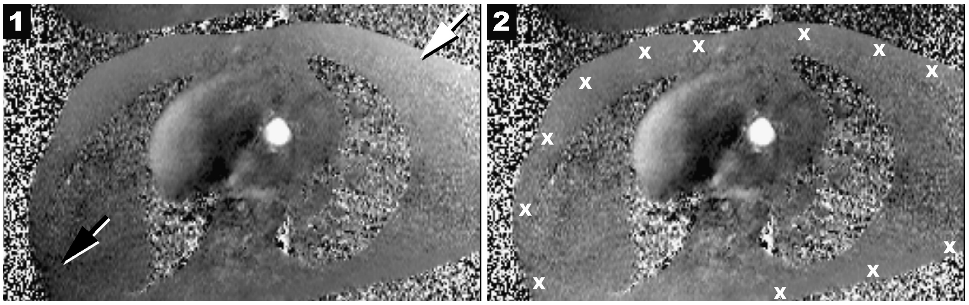

Figure 4. An extreme example of background phase shift. The patient had complex congenital heart disease and moderate aortic valve regurgitation. Panel 1 shows the uncorrected phase image acquired with breath-holding. Background phase shift can be recognized as a change in the signal intensity of stationary tissue, such as the chest wall, from negative (black arrow) to positive (white arrow) across the image. On the uncorrected velocity map, aortic regurgitant fraction is calculated to be 2%. In Panel 2, markers (represented by X) are placed on the chest wall and background correction is applied. Following correction, regurgitant fraction of 24% is obtained. On modern scanners, background phase shift is now much less of a problem.

temporal resolution (number of frames or phases per heart beat) is set too low, flow and peak velocities may be underestimated. The temporal resolution largely depends on the patient's heart rate but can usually be optimized by the user by changing the repetition time, acquisition window, and, if k-space segmentation is employed, the number of views per segment. These parameters are adjusted with consideration to the scan time, particularly with breath-hold acquisitions. Increasing the number of views per segment will reduce the scan time but will also reduce the temporal resolution. For breath-hold acquisitions, we usually acquire 15 to 25 frames per cardiac cycle with a scan time of 15 to 30 seconds and 3 to 5 views per segment, depending on the heart rate. For non-breath-hold velocity mapping, we typically acquire 30 frames per cardiac cycle with a scan time of about 2 minutes without k-space segmentation.

4.4. *Partial volume effects*

The velocity measured in a voxel is a mean value of the range of velocities recorded within that voxel. This mean velocity depends on the relative amplitude and the phase of the signal components in the voxel. If the voxel straddles an area of very high and very low velocities, partial volume averaging ensues, resulting in underestimation of flow and peak velocity. This problem is most pronounced when estimating in-plane peak velocity in a narrow jet with a thick slice (16).

4.5. *Signal loss*

Signal loss may be due to artifacts, such as metallic artifacts from prosthetic valves, and turbulent blood flow. The latter is due to chaotic flow in which the velocity components fluctuate randomly. Phase-contrast velocity mapping is optimized for linear flow and turbulent flow may render flow measurement imprecise or impossible. Reducing the echo time decreases the signal loss due to turbulence (17), and on modern scanners, very short echo times are now available to overcome this problem.

4.6. *Phase offset errors*

Phase offset errors are due to local magnetic field inhomogeneities or gradient imbalance. It appears to be more pronounced with breath-hold acquisitions, perhaps due to Maxwell gradients (18) and eddy currents induced by rapid gradient switching. Manufacturers have begun making hardware and software modifications to avoid or correct these problems. These offset errors are probably tolerable for peak velocity estimation but may affect measurements of regurgitant fraction. For this reason, we usually employ breath-hold acquisition for velocity measurement, and non-breath-hold acquisition for flow quantification. Phase offset errors can be corrected for by applying simple background correction only if background phase is shifted linearly across the image (Fig. 4). Background correction should, however, be used with care as it may result in errors.

4.7. *Potential errors during data analysis*

It is important not to include noise or edge pixels in the vessel contours as these will result in erroneous mean velocity information and hence inaccurate mean flow measurement. For flow quantification, the internal lumen of the vessel should be accurately contoured. Too small a contour results in underestimation of the mean flow. With automated contour detection software, the generated contours must be cross-checked for accuracy and to ensure that noise pixels are not incorporated in the ROI.

5. Typical imaging parameters

The typical settings that we use for phase-contrast velocity mapping are detailed in Table 3.

Table 3. Typical scanner parameters (1.5T Siemens Magnetom Sonata)

Parameters	Non-breath-hold through-plane acquisition	Breath-hold through-plane acquisition	Breath-hold in-plane acquisition
Field of view (FOV)	300–380 mm	300–380 mm	300–400 mm
Voxel size @ 350 mm FOV	1.7 × 1.4 × 8.0 mm	2.1 × 1.4 × 8.0 mm	2.8 × 1.8 × 8.0 mm
Slice thickness	8 mm	8 mm	6 mm
Flip angle	30°	20°	20°
Segments	1	3–5	3–5
Bandwidth	235 Hz/pixel	698 Hz/pixel	766 Hz/pixel
Echo time	4 ms	2.2–3.3 ms	3.8–5.0 ms
Repetition time	20–40 ms	30–60 ms	40–64 ms
Phases	20–30	15–25	15–25
Base resolution	128 × 256	104 × 256	94 × 192
Approximate scan time	2–3 minutes	15–30 seconds	18–32 seconds

6. Practical tips with specific clinical examples

In this section, we provide several clinical examples on how phase-contrast velocity mapping can be helpful in specific acquired and congenital cardiac conditions. All patients were scanned using a 1.5T Siemens Magnetom Sonata scanner (Siemens Medical Solutions, Erlangen, Germany), and data analysis was performed with CMRTools (Cardiovascular Imaging Solutions, London, United Kingdom).

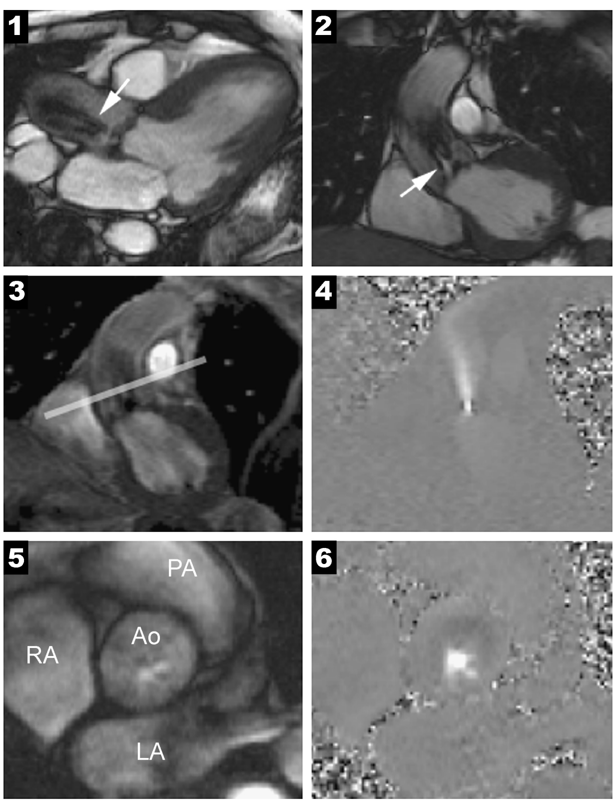

Figure 5. Gradient echo images and velocity mapping of a patient with aortic valve stenosis. Ao, aorta; PA, pulmonary artery; RA, right atrium; LA, left atrium.

6.1. *Example 1: aortic stenosis*

A 76-year old gentleman with dyspnea and aortic valve stenosis (19–21) is referred for CMR study prior to valve replacement surgery (Fig. 5). The left ventricle is hypertrophied and systolic function is preserved. Panels 1 and 2 in Fig. 5 show mid-systolic gradient echo images of the left ventricular outflow tract (LVOT) in the long axis and coronal planes, respectively. The aortic valve appears thickened and severely restricted in systolic excursion. A systolic jet through the stenosed aortic valve can be seen (white arrows) in the aortic root with a bright jet core of coherent flow surrounded by signal loss due to turbulent flow.

In-plane breath-hold velocity mapping of the same image plane as depicted in Panel 2 is performed to visualize the jet.

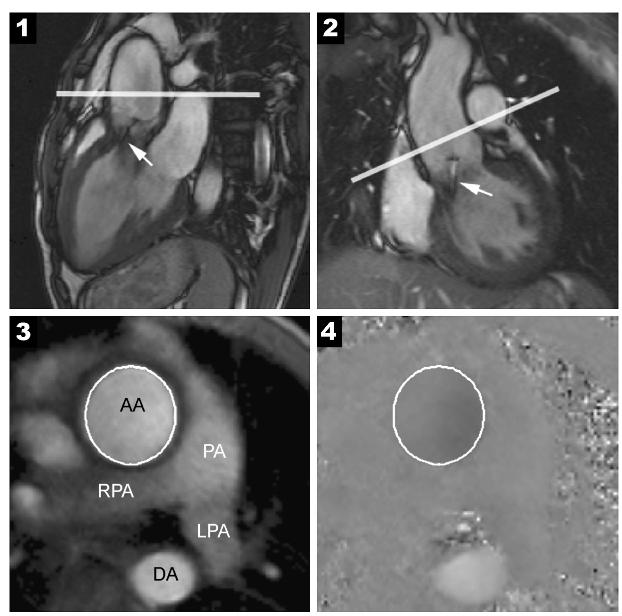

Figure 6. Gradient echo images and velocity mapping of a case with aortic valve regurgitation. AA, ascending aorta; PA, main pulmonary artery; RPA, right pulmonary artery; LPA, left pulmonary artery; DA, descending aorta.

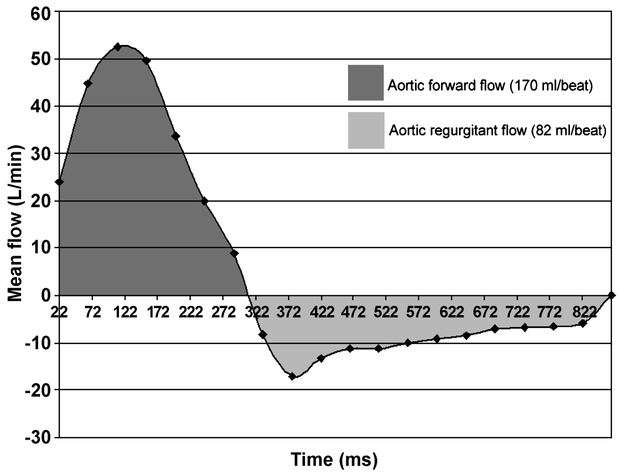

Figure 7. Aortic flow curve in a case of severe aortic valve regurgitation.

Venc is set at 500 cm/s. The in-plane field of view is rotated counter-clockwise to align the velocity-encoding direction (vertically in this case) parallel to the main jet stream. Panel 3 shows the magnitude image in mid-systole, with the corresponding phase image in Panel 4. The bright stenotic jet can be seen clearly in the center of the image.

Breath-hold through-plane acquisitions are then obtained (Panel 5: magnitude image in mid-systole; Panel 6: corresponding phase image). The image plane is perpendicular to the jet stream just above the aortic valve in mid-systole, avoiding the aortic valve itself. The approximate acquisition plane is indicated by the white line in Panel 3. The Venc is initially set at 500 cm/s and the acquisition is repeated with Venc of 450 cm/s. In Panel 6, the central white jet core can be seen. Planimetry of this area approximates the valve area of 0.7 cm^2. Analysis of the pixels in this area shows a peak velocity of 4.3 m/s, corresponding to a maximal pressure gradient of 74 mmHg by the modified Bernoulli equation. These findings are consistent with severe aortic valve stenosis and are indications for valve replacement surgery.

6.2. *Example 2: aortic regurgitation*

The patient is a 38-year old gentleman with annulo-aortic ectasia and aortic valve regurgitation (22–24), and he is referred for CMR assessment of cardiac function and severity of the valve lesion (Fig. 6). Gradient echo cine imaging reveals a dilated aortic root, dilated left ventricle and signal loss from a turbulent eccentric regurgitant jet in the LVOT throughout diastole (arrowed in Panels 1 and 2, which are gradient echo images in early diastole). Left ventricular ejection fraction is 56% by ventricular volume measurement.

Through-plane, non-breath-hold, retrospectively gated velocity mapping is performed with a plane perpendicular to the aortic root at the level of the sino-tubular junction, taking care to avoid the valve plane which moves during the cardiac cycle. Velocity is encoded in a through-plane direction such that blood flowing cranially appears white. Venc is set at 200 cm/s, and 20 frames per cardiac cycle are acquired. Panel 3 shows the magnitude image in early diastole. The internal diameter of the aorta is outlined and the contour is copied and transferred to the corresponding phase image in Panel 4. This is done for all 20 frames. In the phase image, reverse flow in the ascending aorta (AA) during diastole appears as dark pixels. Multiplying the mean velocity and the area planimetered gives the mean flow through the ascending aorta at the particular time frame of the cardiac cycle. Integrating the mean flow for all 20 frames produces a flow volume versus time curve, as illustrated in Fig. 7. The shaded area above the x-axis represents forward stroke volume, which in this case is 170 ml/beat. The shaded area below the x-axis represents regurgitant flow of 82 ml/beat. Regurgitant fraction is thus 48% indicating severe aortic valve regurgitation. Notice that in diastole, the descending aorta (DA) appears white on the phase image (Panel 4 in Fig. 6), indicating diastolic reversal flow, another sign of severe aortic valve regurgitation.

6.3. *Example 3: shunt ratio quantification*

An 18-year old lady who was known to have a 1.5 cm ventricular septal defect (VSD) is referred for re-evaluation of

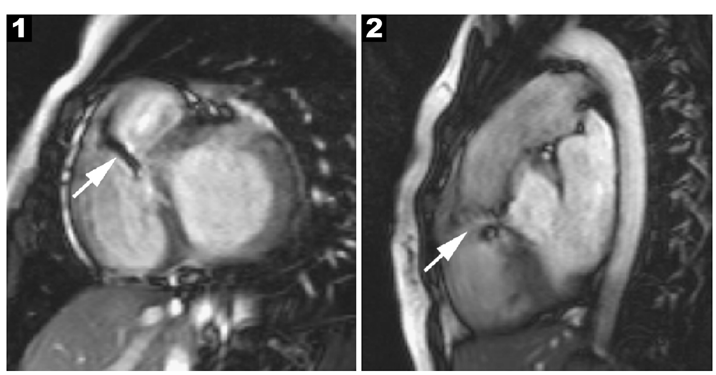

Figure 8. Gradient echo images showing the basal short axis level (Panel 1) and the right ventricular outflow tract (Panel 2) in mid-systole. A defect in the membranous part of the ventricular septum can be appreciated, and a high-velocity systolic jet through the defect is indicated by arrows.

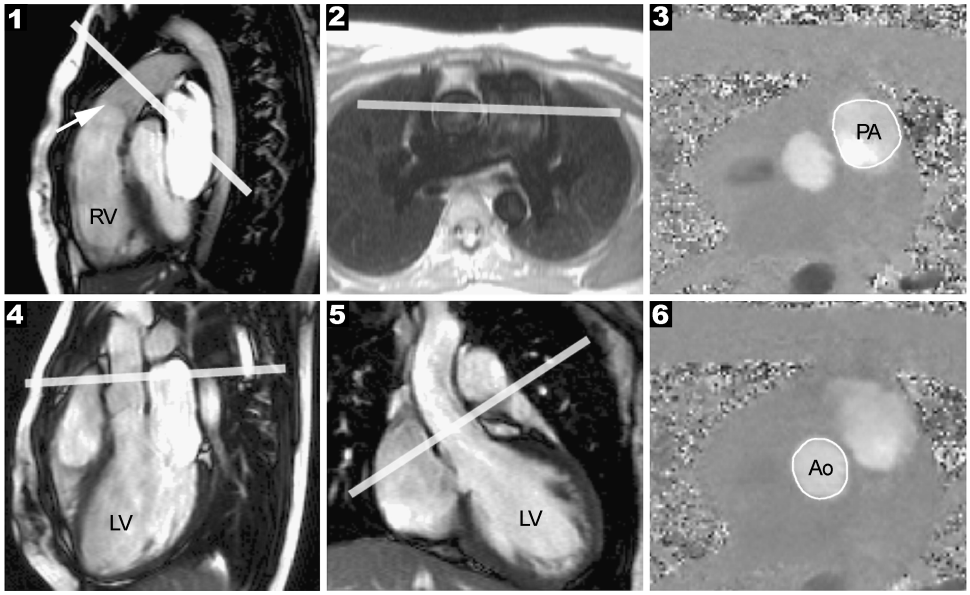

Figure 9. Shunt ratio quantification. RV, right ventricle; LV, left ventricle; PA, pulmonary artery; Ao, aorta.

the septal defect, assessment of ventricular volumes and function, as well as shunt ratio quantification (Qp:Qs) (Figs. 8 and 9). Gradient echo images (Fig. 8) show an obvious perimembranous VSD with a high-velocity jet in the right ventricular outflow tract (RVOT). The pulmonary arteries and left ventricle are mildly dilated, and biventricular systolic function is preserved.

For Qp:Qs measurement (25, 26), two separate acquisitions are obtained for quantification of flow in the main pulmonary artery (PA) and in the aorta. For velocity mapping of the PA, the oblique sagittal view of the RVOT (Panel 1 in Fig. 9) and a transaxial spin echo image showing the PA bifurcation (Panel 2) are used to locate the acquisition plane. Through-plane non-breath-hold velocity mapping is performed in a plane that transects the PA between the pulmonary valve (arrowed, Panel 1 in Fig. 9) and the PA bifurcation. The approximate acquisition plane is indicated by the white lines in Panels 1 and 2. Venc is set at 150 cm/s. Panel 3 shows one of the phase images obtained. The internal circumference of the PA is contoured as shown. For aortic flow, through-plane, non-breath-hold, retrospectively gated velocity mapping is performed at the sinotubular junction with Venc set at 180 cm/s. The imaging plane is indicated by the white lines in Panels 4 and 5 in Fig. 9. Panel 6 shows one of the phase images with the internal circumference of the aorta delineated. Data analysis produces the flow versus time curves shown in Fig. 10. In this patient, right ventricular stroke volume (PA flow) is 156 ml/beat and left ventricular stroke volume (aortic flow) is 71 ml/beat, giving a Qp:Qs of 2.2. This is consistent with a large shunt and is an indication for surgical intervention in this patient.

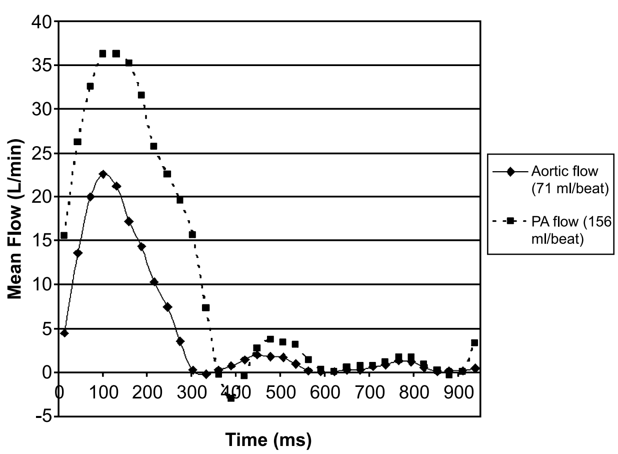

Figure 10. Aortic and pulmonary flow versus time curves.

6.4. *Example 4: aortic coarctation*

CMR is perhaps the most ideal imaging modality for studying aortic coarctation because of its unrestricted access to the chest, its non-invasive nature, and its ability to provide anatomic and flow information (27, 28) (Fig. 11). A 19-year old gentleman who is known to have aortic coarctation and mildly stenotic bicuspid aortic valve is referred for evaluation. He had previously undergone 2 attempts at balloon dilatation. Preliminary gradient echo imaging clearly demonstrates re-coarctation. As shown in Panels 1 and 3 in Fig. 11, a narrow jet of signal loss (indicated by arrowheads) can be seen on gradient echo images in mid-systole, originating from a constriction (arrowed) at the distal aortic arch. Images are acquired in several oblique sagittal and coronal planes. Notice also that the ascending aorta is dilated.

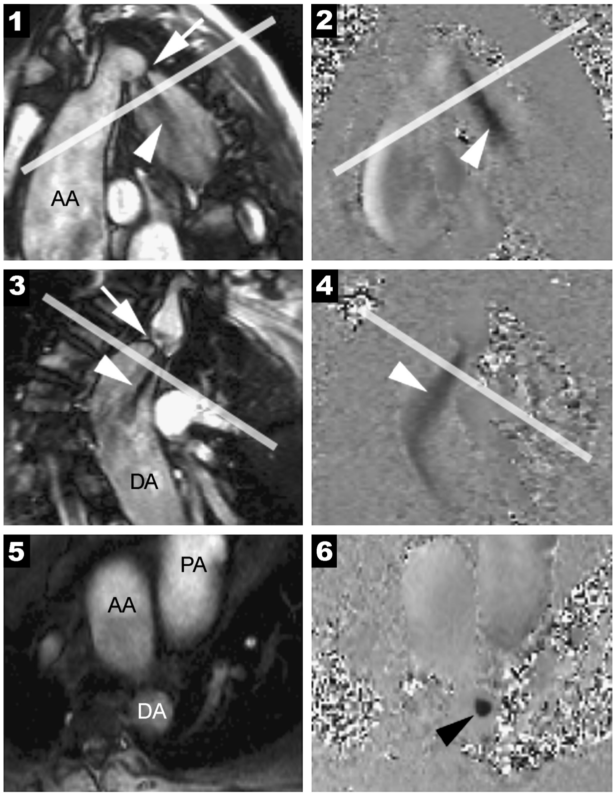

Figure 11. Gradient echo images and velocity mapping of a patient with aortic coarctation. DA, descending aorta; LV, left ventricle; AA, ascending aorta.

In-plane breath-hold velocity mapping is performed, copying the image positions shown in Panels 1 and 3. Panels 2 and 4 illustrate the resultant phase images. The black pixels (indicated by white arrowheads) in the descending aorta (DA) represent the coarctation jet stream. Peak velocity estimation can be made on this image but because the jet is narrow, the measurement may not be reliable due to partial volume effects and the movement of the jet in and out of the imaging plane. Therefore through-plane velocity mapping is also performed. The in-plane phase map may also be examined for persistent flow through the coarctation into the diastolic phase of the cardiac cycle (diastolic tailing), an indication of significant stenosis.

In this patient, through-plane velocity mapping is done with breath-hold and retrospective gating. Venc is set at 400 cm/s initially. The imaging plane, indicated by the white lines in Panels 1 to 4, is positioned below the narrowest point of the jet to avoid signal loss from turbulent flow and eddy currents. It is oriented perpendicular to the jet. The resultant magnitude and phase images in mid-systole are shown in Panels 5 and 6, respectively. Several through-plane acquisitions may be made above and below this imaging plane in order to determine the region with the highest velocity. The dark pixels (indicated by black arrowhead in Panel 6) on the phase image represent the jet core. In this case, peak velocity is 3.3 m/s, giving a calculated maximal pressure gradient of 43 mmHg across the stenosis, consistent with significant re-coarctation.

A useful application of flow measurement in coarctation is the assessment of collateral flow. Through-plane velocity maps of the DA just distal to the coarctation site and at the level of the diaphragm can be obtained and flow at these sites quantified. Normally, flow in the distal aortic arch is slightly higher than that in the descending thoracic aorta. With significant coarctation, this is reversed, with increased flow at the level of the diaphragm due to collateral circulation (29, 30).

6.5. *Example 5: repaired tetralogy of fallot*

Phase-contrast velocity mapping is often employed in the assessment of congenital heart disease for shunt quantification, determination of regurgitant fraction and velocity measurement in the presence of arterial, valvular, or venous stenosis (31–38) (Fig. 12). The patient is a 21-year old lady with tetralogy of Fallot repaired in childhood. She is referred for assessment of pulmonary regurgitation (PR), a common complication of early repair procedure. Initial gradient echo imaging reveals a mildly dilated right ventricle with preserved ejection fraction, significant PR, and right pulmonary artery stenosis.

Panel 1 in Fig. 12 shows a transaxial gradient echo image at the level of the pulmonary artery bifurcation. The stenosed segment of the right pulmonary artery (RPA) is indicated by the black arrowhead. Turbulent flow downstream from the stenosis is seen as a jet of signal loss (white arrowhead). Through-plane breath-hold velocity mapping is performed with the imaging plane indicated by the white line in Panel 1. Venc is set at 400 cm/s and the acquisition is later repeated with a Venc of 350 cm/s. On the magnitude (Panel 2) and phase (Panel 3) images, the jet can be seen as dark regions indicated by arrowheads. Peak velocity is 3 m/s, consistent with moderate stenosis of the RPA. The left pulmonary artery (LPA) is patent.

Panel 4 illustrates the right ventricular outflow tract (RVOT) in the oblique sagittal plane in early diastole on gradient echo imaging. Pulmonary regurgitation is seen as a jet of signal loss indicated by the white arrowhead. There is no functioning pulmonary valve. Non-breath-hold through-plane velocity mapping is performed with a plane (indicated by white line) between the pulmonary artery (PA) bifurcation and the site of the pulmonary valve for quantification of regurgitant fraction. Venc is set at 150 cm/s. In this patient, the pulmonary regurgitant fraction is quantified as 37%. This can be considered as almost free pulmonary regurgitation. CMR is an ideal tool for following up this patient with serial determinations of right ventricular function and pulmonary regurgitant fraction as well as progression of the RPA stenosis, so that surgical intervention can be carried out before right ventricular function deteriorates significantly.

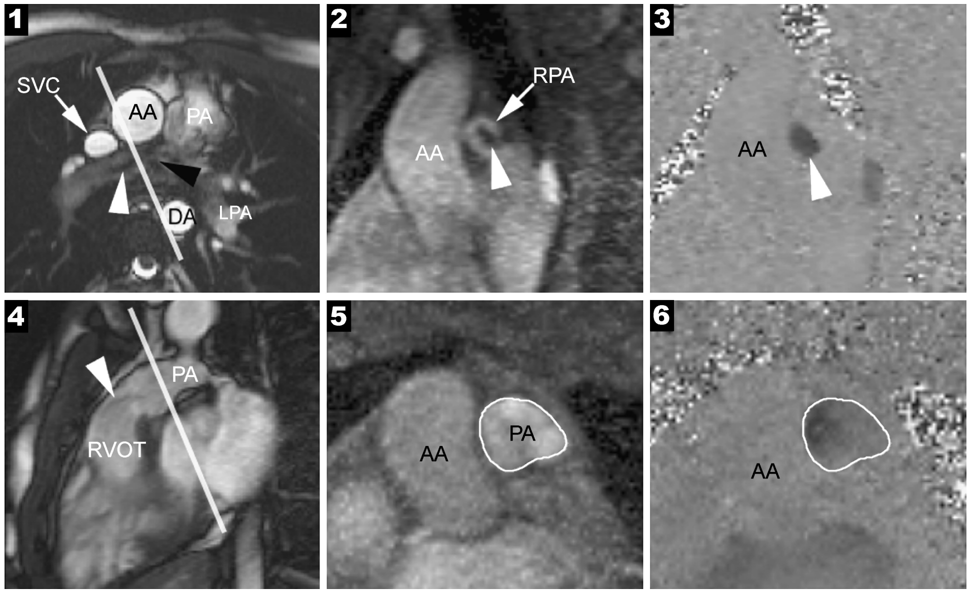

Figure 12. Gradient echo images (Panels 1 and 4), magnitude images (Panels 2 and 5) and corresponding phase images (Panels 3 and 6) in a patient who had undergone previous surgical repair for tetralogy of Fallot. SVC, superior vena cava; AA, ascending aorta; PA, pulmonary artery; RPA, right pulmonary artery; LPA, left pulmonary artery; DA, descending aorta; RVOT, right ventricular outflow tract.

7. Conclusion

Phase-contrast velocity mapping is a versatile method of assessing flow and velocity which can make important contributions to a comprehensive cardiovascular magnetic resonance study. Accuracy depends, however, on appropriate hardware, software, image acquisition and data analysis. With experience, and with the limitations and pitfalls of the method in mind, reliable flow data that will help in the diagnosis, treatment and follow-up of the patient can be derived.

Acknowledgments

The authors would like to thank Dr. Philip Kilner and Peter Gatehouse for proofreading the manuscript and Professor David Firmin for his help. The authors would also like to acknowledge the Royal Brompton & Harefield NHS Trust, the British Heart Foundation, and CORDA The Heart Charity for providing support and grants.

References

1. Firmin D. Blood flow velocity assessment. In: Manning WJ, Pennell DJ, eds. Cardiovascular Magnetic Resonance. Philadelphia: Churchill Livingstone, 2002: 53–62.
2. Firmin DN, Nayler GL, Klipstein RH, Underwood SR, Rees RS, Longmore DB. In vivo validation of MR velocity imaging. J Comput Assist Tomogr 1987; 11:751–756.
3. Hoeper MM, Tongers J, Leppert A, Baus S, Maier R, Lotz J. Evaluation of right ventricular performance with a right ventricular ejection fraction thermodilution catheter and MRI in patients with pulmonary hypertension. Chest 2001; 120:502–507.
4. Kondo C, Caputo GR, Semelka R, Foster E, Shimakawa A, Higgins CB. Right and left ventricular stroke volume measurements with velocity-encoded cine MR imaging: in vitro and in vivo validation. AJR, Am J Roentgenol 1991; 157:9–16.
5. Lee VS, Spritzer CE, Carroll BA, Pool LG, Bernstein MA, Heinle SK, MacFall JR. Flow quantification using fast cine phase-contrast MR imaging, conventional cine phase-contrast MR imaging, and Doppler sonography: in vitro and in vivo validation. AJR, Am J Roentgenol 1997; 169:1125–1131.
6. Mohiaddin RH, Pennell DJ. MR blood flow measurement. Clinical application in the heart and circulation. Cardiol Clin 1998; 16:161–187.
7. Tan RS, Mohiaddin RH. Cardiovascular applications of magnetic resonance flow measurement. Rays 2001; 26:71–91.
8. O'Donnell M. NMR blood flow imaging using multiecho, phase contrast sequences. Med Phys 1985; 12:59–64.
9. Spritzer CE, Pelc NJ, Lee JN, Evans AJ, Sostman HD, Riederer SJ. Rapid MR imaging of blood flow with a phase-sensitive, limited-flip-angle, gradient recalled pulse sequence: preliminary experience. Radiology 1990; 176:255–262.
10. Mohiaddin RH, Gatehouse PD, Firmin DN. Exercise-related changes in aortic flow measured with spiral echo-planar MR velocity mapping. J Magn Reson Imaging 1995; 5:159–163.
11. Lotz J, Meier C, Leppert A, Galanski M. Cardiovascular flow measurement with phase-contrast MR imaging: basic facts and implementation. Radiographics 2002; 22:651–671.
12. Sakuma H, Kawada N, Kubo H, Nishide Y, Takano K, Kato N, Takeda K. Effect of breath holding on blood flow measurement using fast velocity encoded cine MRI. Magn Reson Med 2001; 45:346–348.
13. Mohiaddin RH, Kilner PJ. Valvular heart disease. In: Manning WJ, Pennell DJ, eds. Cardiovascular Magnetic Resonance. Philadelphia: Churchill Livingstone, 2002, 387–404.
14. Andersen AH, Kirsch JE. Analysis of noise in phase contrast MR imaging. Med Phys 1996; 23:857–869.
15. Yang GZ, Burger P, Kilner PJ, Karwatowski SP, Firmin DN. Dynamic range extension of cine velocity measurements using

motion-registered spatiotemporal phase unwrapping. J Magn Reson Imaging 1996; 6:495–502.
16. Tang C, Blatter DD, Parker DL. Accuracy of phase-contrast flow measurements in the presence of partial-volume effects. J Magn Reson Imaging 1993; 3:377–385.
17. Kilner PJ, Firmin DN, Rees RS, Martinez J, Pennell DJ, Mohiaddin RH, Underwood SR, Longmore DB. Valve and great vessel stenosis: assessment with MR jet velocity mapping. Radiology 1991; 178:229–235.
18. Bernstein MA, Zhou XJ, Polzin JA, King KF, Ganin A, Pelc NJ, Glover GH. Concomitant gradient terms in phase contrast MR: analysis and correction. Magn Reson Med 1998; 39:300–308.
19. Caruthers SD, Lin SJ, Brown P, Watkins MP, Williams TA, Lehr KA, Wickline SA. Practical value of cardiac magnetic resonance imaging for clinical quantification of aortic valve stenosis: comparison with echocardiography. Circulation 2003; 108:2236–2243.
20. Kilner PJ, Manzara CC, Mohiaddin RH, Pennell DJ, Sutton MG, Firmin DN, Underwood SR, Longmore DB. Magnetic resonance jet velocity mapping in mitral and aortic valve stenosis. Circulation 1993; 87:1239–1248.
21. Sondergaard L, Hildebrandt P, Lindvig K, Thomsen C, Stahlberg F, Kassis E, Henriksen O. Valve area and cardiac output in aortic stenosis: quantification by magnetic resonance velocity mapping. Am Heart J 1993; 126:1156–1164.
22. Chatzimavroudis GP, Oshinski JN, Franch RH, Pettigrew RI, Walker PG, Yoganathan AP. Quantification of the aortic regurgitant volume with magnetic resonance phase velocity mapping: a clinical investigation of the importance of imaging slice location. J Heart Valve Dis 1998; 7:94–101.
23. Didier D. Assessment of valve disease: qualitative and quantitative. Magn Reson Imaging Clin N Am 2003; 11:115–134.
24. Dulce MC, Mostbeck GH, O'Sullivan M, Cheitlin M, Caputo GR, Higgins CB. Severity of aortic regurgitation: interstudy reproducibility of measurements with velocity-encoded cine MR imaging. Radiology 1992; 185:235–240.
25. Beerbaum P, Korperich H, Barth P, Esdorn H, Gieseke J, Meyer H. Noninvasive quantification of left-to-right shunt in pediatric patients: phase-contrast cine magnetic resonance imaging compared with invasive oximetry. Circulation 2001; 22:2476–2482.
26. Brenner LD, Caputo GR, Mostbeck G, Steiman D, Dulce M, Cheitlin MD, O'Sullivan M, Higgins CB. Quantification of left to right atrial shunts with velocity-encoded cine nuclear magnetic resonance imaging. J Am Coll Cardiol 1992; 20:1246–1250.
27. Engvall J, Sjoqvist L, Nylander E, Thuomas KA, Wranne B. Biplane transoesophageal echocardiography, transthoracic Doppler, and magnetic resonance imaging in the assessment of coarctation of the aorta. Eur Heart J 1995; 16:1399–1409.
28. Mohiaddin RH, Kilner PJ, Rees S, Longmore DB. Magnetic resonance volume flow and jet velocity mapping in aortic coarctation. J Am Coll Cardiol 1993; 22:1515–1521.
29. Holmqvist C, Stahlberg F, Hanseus K, Hochbergs P, Sandstrom S, Larsson EM, Laurin S. Collateral flow in coarctation of the aorta with magnetic resonance velocity mapping: correlation to morphological imaging of collateral vessels. J Magn Reson Imaging 2002; 15:39–46.
30. Steffens JC, Bourne MW, Sakuma H, O'Sullivan M, Higgins CB. Quantification of collateral blood flow in coarctation of the aorta by velocity encoded cine magnetic resonance imaging. Circulation 1994; 90:937–943.
31. Boxt LM, Rozenshtein A. MR imaging of congenital heart disease. Magn Reson Imaging Clin N Am 2003; 11:27–48.
32. Davlouros PA, Kilner PJ, Hornung TS, Li W, Francis JM, Moon JC, Smith GC, Tat T, Pennell DJ, Gatzoulis MA. Right ventricular function in adults with repaired tetralogy of Fallot assessed with cardiovascular magnetic resonance imaging: detrimental role of right ventricular outflow aneurysms or akinesia and adverse right-to-left ventricular interaction. J Am Coll Cardiol 2002; 40:2044–2052.
33. Helbing WA, de Roos A. Clinical applications of cardiac magnetic resonance imaging after repair of tetralogy of Fallot. Pediatr Cardiol 2000; 21:70–79.
34. Helbing WA, Niezen RA, Le Cessie S, van der Geest RJ, Ottenkamp J, de Roos A. Right ventricular diastolic function in children with pulmonary regurgitation after repair of tetralogy of Fallot: volumetric evaluation by magnetic resonance velocity mapping. J Am Coll Cardiol 1996; 28:1827–1835.
35. Li W, Davlouros PA, Kilner PJ, Pennell DJ, Gibson D, Henein MY, Gatzoulis MA. Doppler-echocardiographic assessment of pulmonary regurgitation in adults with repaired tetralogy of Fallot: comparison with cardiovascular magnetic resonance imaging. Am Heart J 2004; 147:165–172.
36. Niezen RA, Helbing WA, van der Wall EE, van der Geest RJ, Rebergen SA, de Roos A. Biventricular systolic function and mass studied with MR imaging in children with pulmonary regurgitation after repair for tetralogy of Fallot. Radiology 1996; 201:135–140.
37. Rebergen SA, Chin JG, Ottenkamp J, van der Wall EE, de Roos A. Pulmonary regurgitation in the late postoperative follow-up of tetralogy of Fallot. Volumetric quantitation by nuclear magnetic resonance velocity mapping. Circulation 1993; 88:2257–2266.
38. Varaprasathan GA, Araoz PA, Higgins CB, Reddy GP. Quantification of flow dynamics in congenital heart disease: applications of velocity-encoded cine MR imaging. Radiographics 2002; 22:895–905.